Observation of Gamma-ray Emission Above 10 TeV from the Super Nova Remnant G106.3+2.7 with the Tibet Air Shower Array and the Muon Detector Array

T. K. Sako
for the Tibet ASγ Collaboration
26 July, 2019 @ ICRC 2019
GAI4b

The Tibet ASγ Collaboration

M. Amenomori(1), Y.-W. Bao(2), X. J. Bi(3), D. Chen(4), T. L. Chen(5), W. Y. Chen(3), Xu Chen(3), Y. Chen(2), Cirennima(5), S. W. Cui(7), Danzengluobu(5), L. K. Ding(3), J. H. Fang(3,6), K. Fang(3), C. F. Feng(8), Zhaoyang Feng(3), Z. Y. Feng(9), Qi Gao(5), Q. B. Gou(3), Y. Y. Guo(3), Y. Q. Guo(3), H. H. He(3), Z. T. He(7), K. Hibino(10), N. Hotta(11), Haibing Hu(5), H. B. Hu(3), J. Huang(3), H. Y. Jia(9), L.Jiang(3), H.-B. Jin(4), F. Kajino(12), K. Kasahara(13), Y. Katayose(14), C. Kato(15) S. Kato(16), K. Kawata(16), W. Kihara(15), Y. Ko(15), M. Kozai(17), Labaciren(5), G. M. Le(18), A. F. Li(19,8,3), H. J. Li(5), W. J. Li(3,9), Y.-H. Lin(3,6), B. Liu(2), C. Liu(3), J. S. Liu(3), M. Y. Liu(5), W. Liu(3), Y.-Q. Lou(20), H.Lu(3), X. R. Meng(5), H. Mitsui(14), K. Munakata(15), H. Nakada(14), Y. Nakamura(3), H. Nanjo(1), M. Nishizawa(21), M. Ohnishi(16), T. Ohura(14), S. Ozawa(22), X. L. Qian(23), X. B. Qu(24), T. Saito(25), M. Sakata(12), T. K. Sako(16), Y. Sengoku(14), J. Shao(3,8), M. Shibata(14), A. Shiomi(26), H. Sugimoto(27), W. Takano(10), M. Takita(16), Y. H. Tan(3), N. Tateyama(10), S. Torii(28), H. Tsuchiya(29), S. Udo(10), H. Wang(3), H. R. Wu(3), L. Xue(8), K. Yagisawa(14), Y. Yamamoto(12), Z. Yang(3), Y. Yokoe(16), A. F. Yuan(5), L. M. Zhai(4), H. M. Zhang(3), J. L. Zhang(3), X. Zhang(2), X. Y. Zhang(8), Y. Zhang(3), Yi Zhang(3), Ying Zhang(3), S. P. Zhao(3), Zhaxisangzhu(5) and X. X. Zhou(9)

(1) Department of Physics, Hirosaki University, Hirosaki 036-8561, Japan
(2) School of Astronomy and Space Science, Nanjing University, Nanjing 210093, China
(3) Key Laboratory of Particle Astrophysics, Institute of High Energy Physics, Chinese Academy of Sciences, Beijing 100049, China
(4) National Astronomical Observatories, Chinese Academy of Sciences, Beijing 100012, China
(5) Physics Department of Science School, Tibet University, Lhasa 850000, China
(6) University of Chinese Academy of Sciences, Beijing 100049, China
(7) Department of Physics, Hebei Normal University, Shijiazhuang 050016, China
(8) Department of Physics, Shandong University, Jinan 250100, China
(9) Institute of Modern Physics, SouthWest Jiaotong University, Chengdu 610031, China
(10) Faculty of Engineering, Kanagawa University, Yokohama 221-8686, Japan
(11) Utsunomiya University, Utsunomiya 321-8505, Japan
(12) Department of Physics, Konan University, Kobe 658-8501, Japan
(13) Shibaura Institute of Technology, Saitama 337-8570, Japan
(14) Faculty of Engineering, Yokohama National University, Yokohama 240-8501, Japan
(15) Department of Physics, Shinshu University, Matsumoto 390-8621, Japan
(16) Institute for Cosmic Ray Research, University of Tokyo, Kashiwa 277-8582, Japan
(17) Institute of Space and Astronautical Science, Japan Aerospace Exploration Agency (ISAS/JAXA), Sagamihara 252-5210, Japan
(18) National Center for Space Weather, China Meteorological Administration, Beijing 100081, China
(19) School of Information Science and Engineering, Shandong Agriculture University, Taian 271018, China
(20) Physics Department, Astronomy Department and Tsinghua Center for Astrophysics, Tsinghua-National Astronomical Observatories of China joint Research Center for Astrophysics, Tsinghua University, Beijing 100084, China
(21) National Institute of Informatics, Tokyo 101-8430, Japan
(22) Advanced ICT Research Institute, National Institute of Information and Communication Technology, Koganei 184-8795, Japan
(23) Department of Mechanical and Electrical Engineering, Shandong Management University, Jinan 250357, China
(24) College of Science, China University of Petroleum, Qingdao, 266555, China
(25) Tokyo Metropolitan College of Industrial Technology, Tokyo 116-8523, Japan
(26) College of Industrial Technology, Nihon University, Narashino 275-8576, Japan
(27) Shonan Institute of Technology, Fujisawa 251-8511, Japan
(28) Research Institute for Science and Engineering, Waseda University, Tokyo 169-8555, Japan
(29) Japan Atomic Energy Agency, Tokai-mura 319-1195, Japan

Tibet Air Shower Array

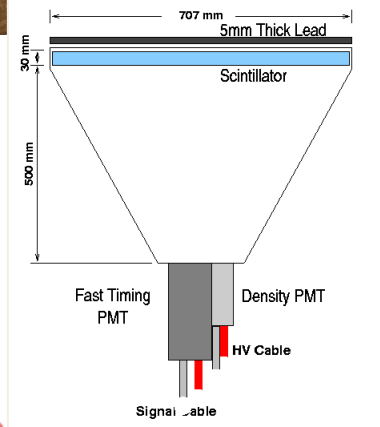

- Tibet, China (90.522°E, 30.102°N) 4,300 m a.s.l.

- scintillation counters 0.5 m^2 x 597
- area ~65,700 m^2
- angular resolution ~0.5°@10TeV
  ~0.2°@100TeV
- energy resolution ~40%@10TeV
  ~20%@100TeV

2nd particles timing ➡ arrival direction
2nd particles energy deposit ➡ primary energy

Water Cherenkov Muon Detector Array

- ✓ 2.4m underground (515g/cm^2 ~19X_0)
- ✓ 7.35m x 7.35m x 1.5m-deep water cell x 64
- ✓ 20”ΦPMT (HAMAMATSU R3600)
- ✓ Concrete pools + Tyvek sheets

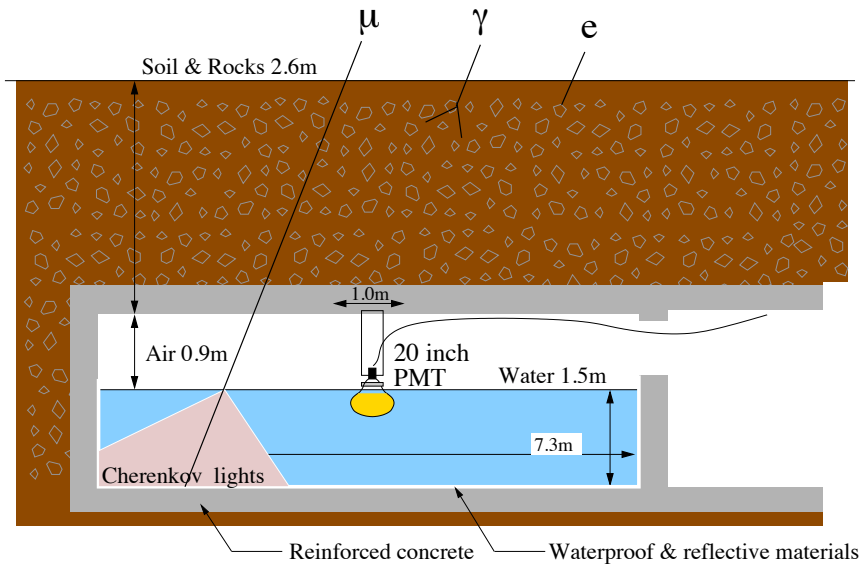

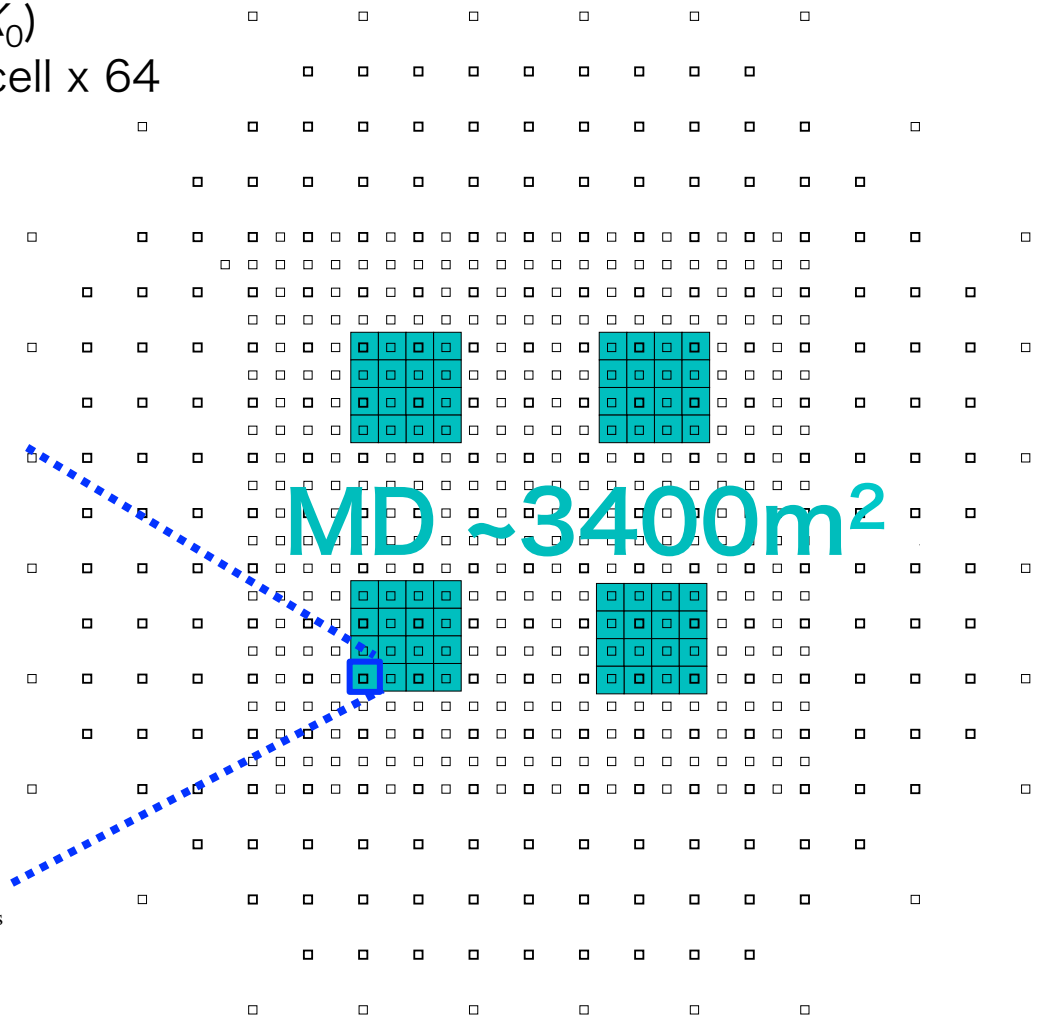

Measurement of number of muons in air showers
➡ γ／CR discrimination

Event selection by MD

Optimization of muon cut

γ : MC sample (Crab orbit & Crab flux)

CR : Data (excluding Crab & Galactic Plane)

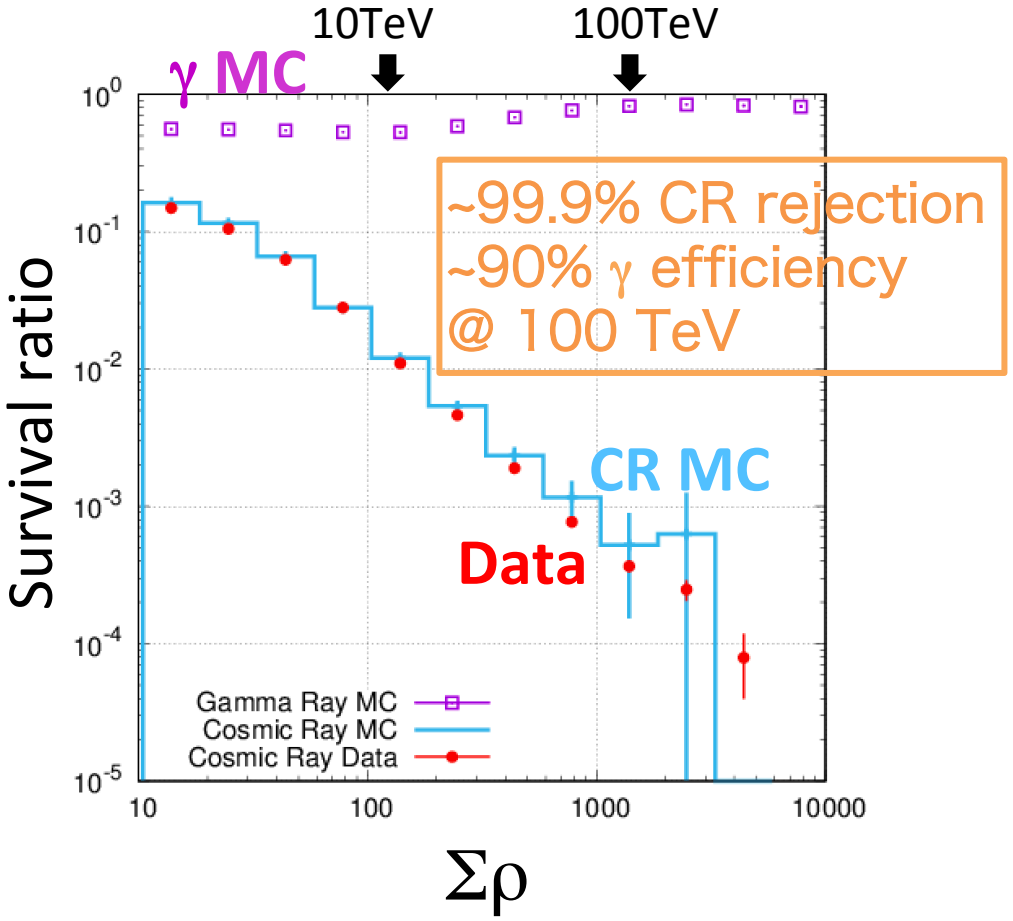

(Sum of particle densities by all AS counters)

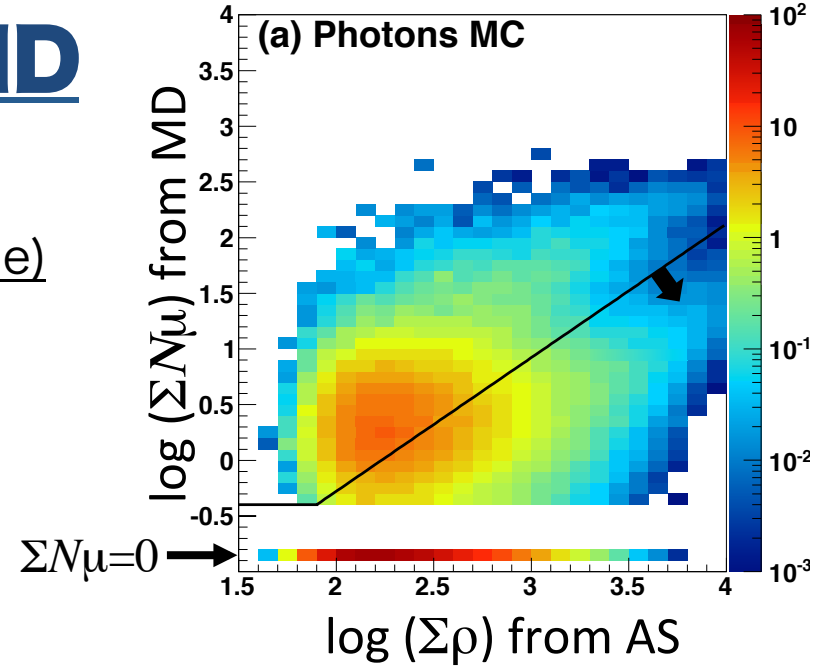

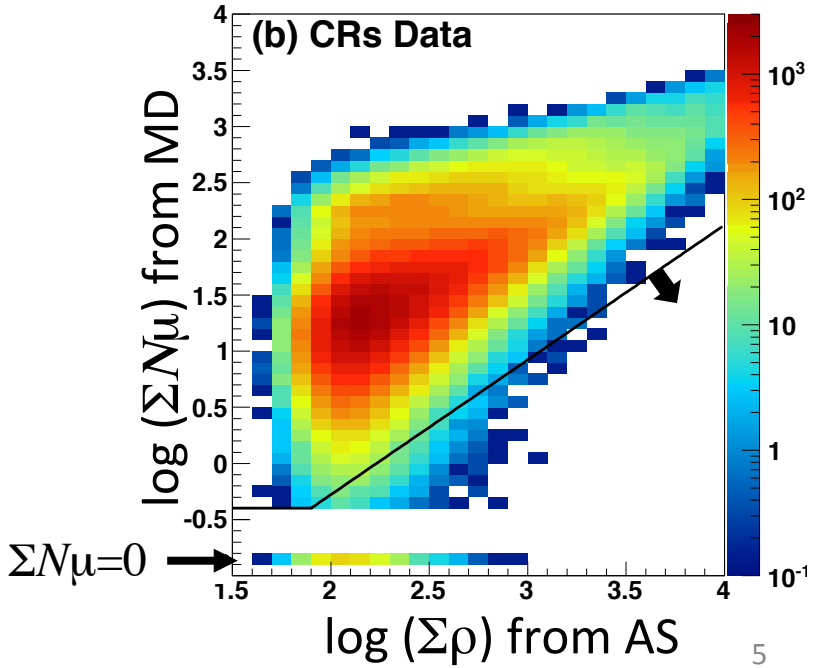

M. Amenomori et al., arXiv:1906.05521 (2019), Accepted by PRL

Crab: γ-like event display

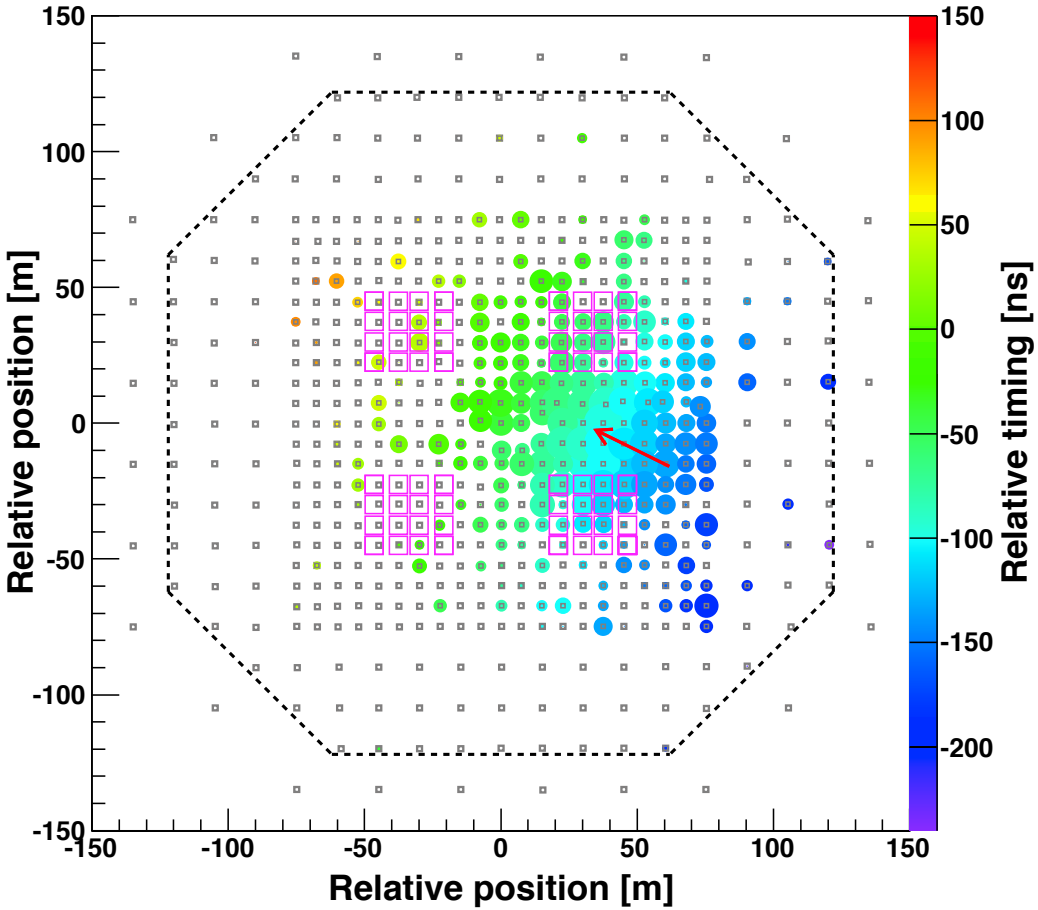

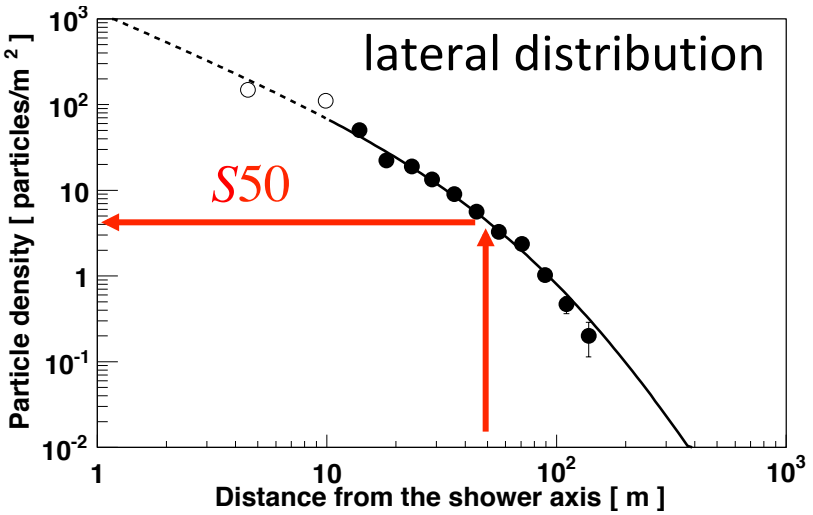

fitting with NKG function

➡ $E_{\rm rec}$ ($S50$, θ)

$\Sigma\rho$ (from AS array) : 3256

$\Sigma N\mu$ (MD) : 2.3

zenith angle : 29.8°

$E_{\rm rec}$: 251^{+46}_{-43} TeV

circle size ∝ log(# of detected particles)

circle color ∝ relative timing [ns]

M. Amenomori et al., arXiv:1906.05521 (2019), Accepted by PRL

Kawata+, Experimental Astronomy, 44, 1 (2017)

Excess count estimation

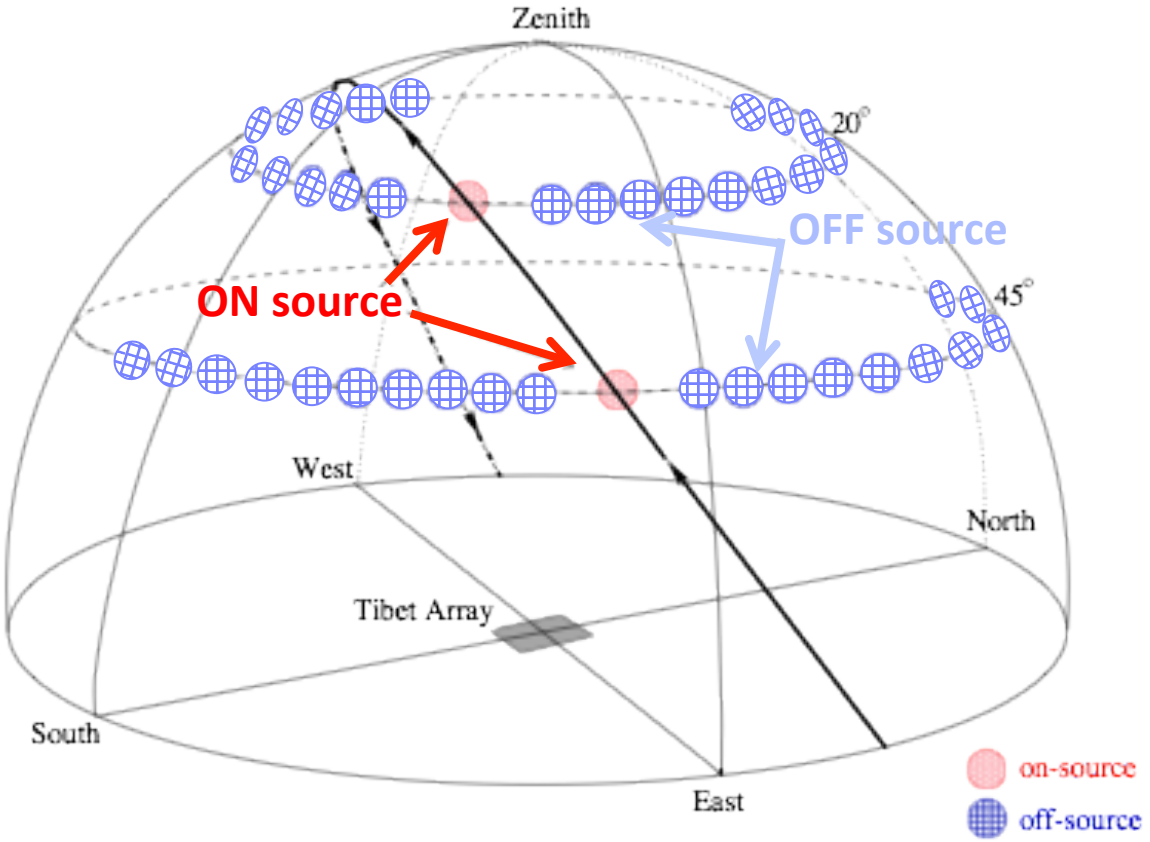

- Data: Feb. 2014 — May 2017 Live time: 720 days
- Standard event selection conditions for AS analysis & **muon cut by MD**
- Equi-Zenith-Angle Method
  - Search window radius (~0.7° to lower limit 0.5°, variable as $R_{\mathrm{SW}} = 6.9^{\circ}/\sqrt{\Sigma\rho}$)
  - N_{ON} : number of events observed in ON-source window
  - $\langle N_{\mathrm{OFF}} \rangle$: average of numbers of events in 20 OFF sources
  - Excess = $N_{\mathrm{ON}} - \langle N_{\mathrm{OFF}} \rangle$

γ-ray emission from Crab

significance map

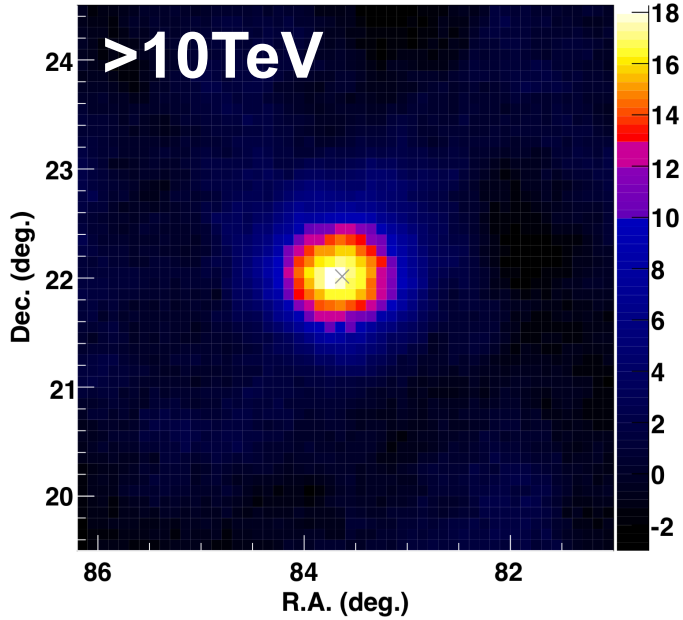

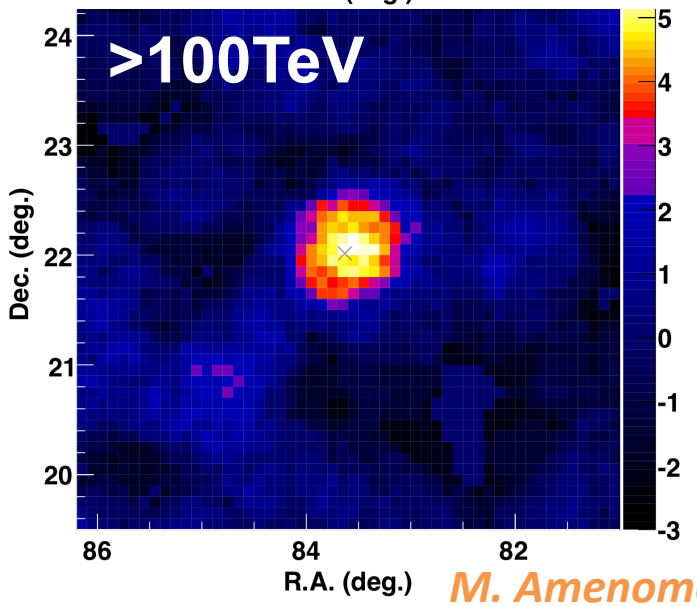

Data vs MC

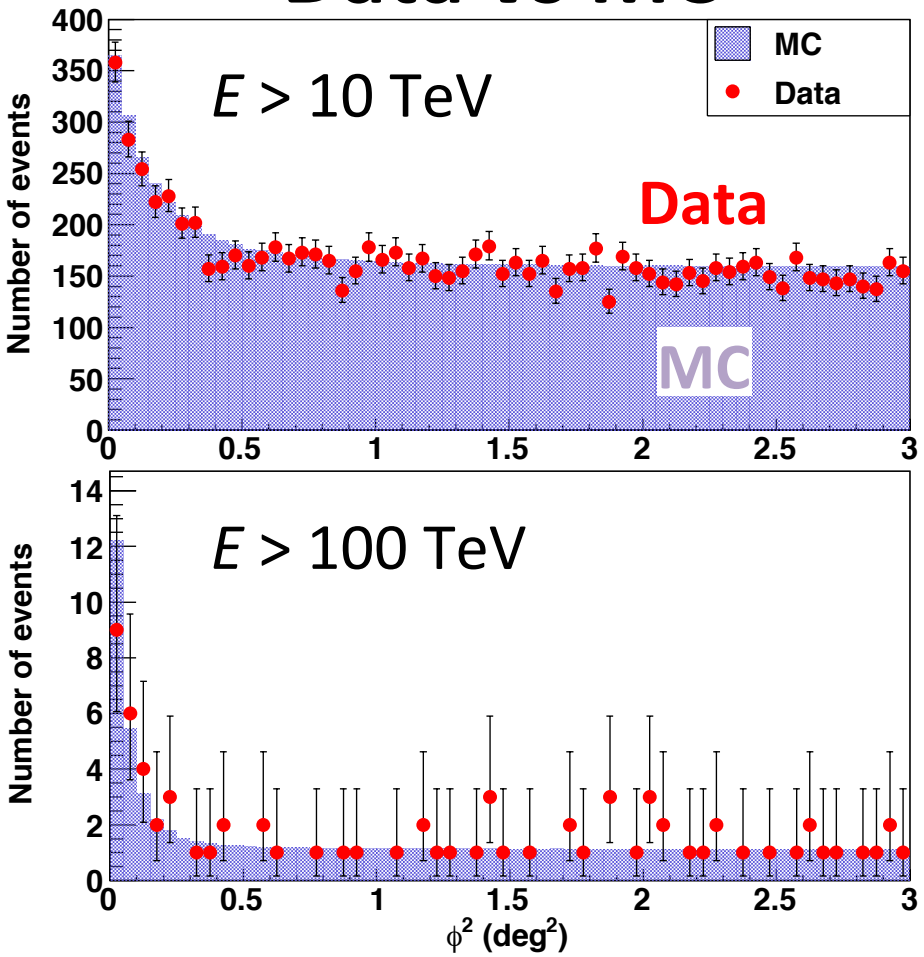

ϕ^2 distributions: consistent with point source

M. Amenomori et al., arXiv:1906.05521 (2019), Accepted by PRL

Number of events (integral)

Crab

Relative number of muons > 100 TeV

E_{Rec}(TeV)	after muon cut	
	N_{ON} / $\langle N_{OFF} \rangle$	σ
>10.0	1691 / 1031	18.3
>15.8	915 / 472.7	17.5
>25.1	417 / 159.1	16.4
>39.8	169 / 46.9	13.2
>63.1	69 / 14.6	9.8
>100	**24 / 5.5**	**5.6**
>251	4 / 0.8	2.4

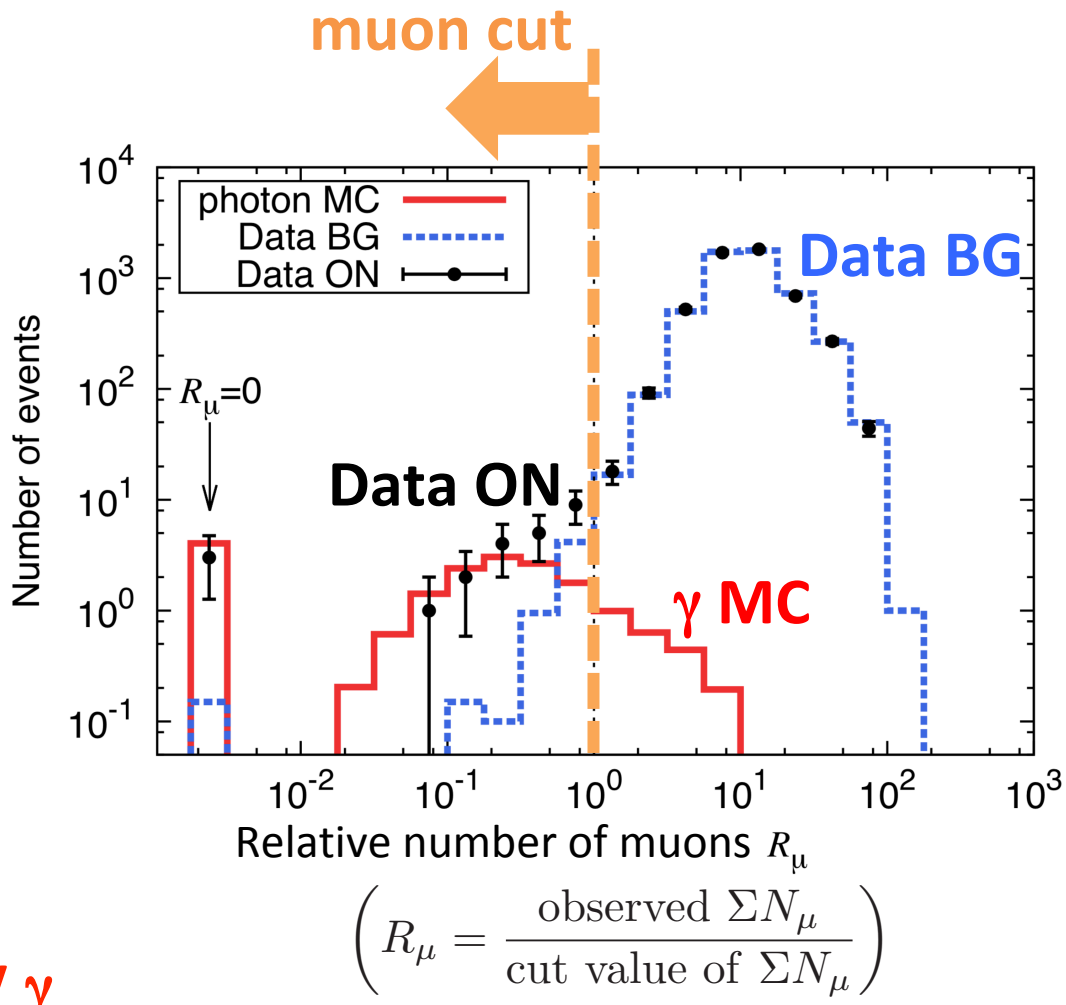

- **First Detection of sub-PeV γ**
- **Highest-energy photon ~450 TeV (*See poster: PS1-75*)**

M. Amenomori et al., arXiv:1906.05521 (2019), Accepted by PRL

γ-ray energy spectrum from Crab

Tibet AS+MD

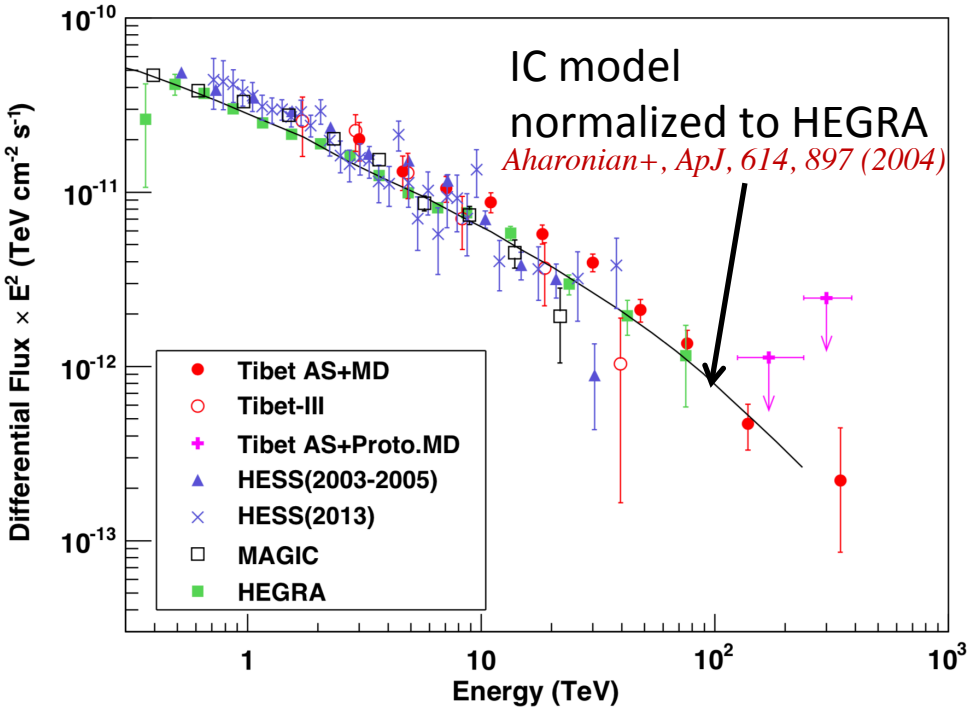

M. Amenomori et al., arXiv:1906.05521

Accepted by PRL (See poster: PS1-75)

E > 100 TeV: 5.6σ

HAWC

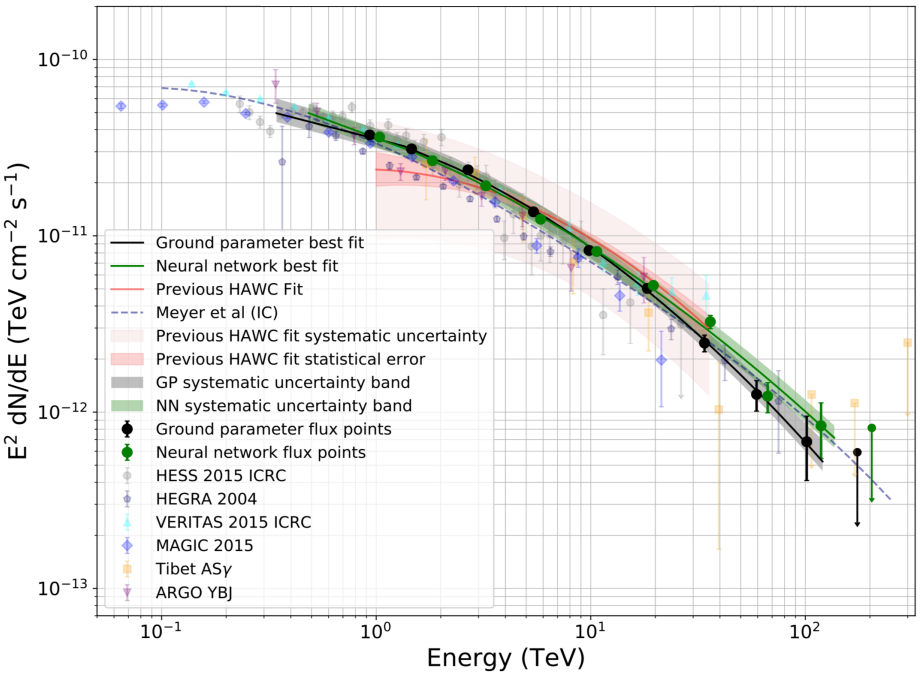

A.U. Abeysekara et al., arXiv:1905.12518

Submitted to ApJ

E > 100 TeV: 3.3σ

spectrum consistent with HAWC recent results

SNR G106.3+2.7

Excess count map > 0.63 TeV by VERITAS

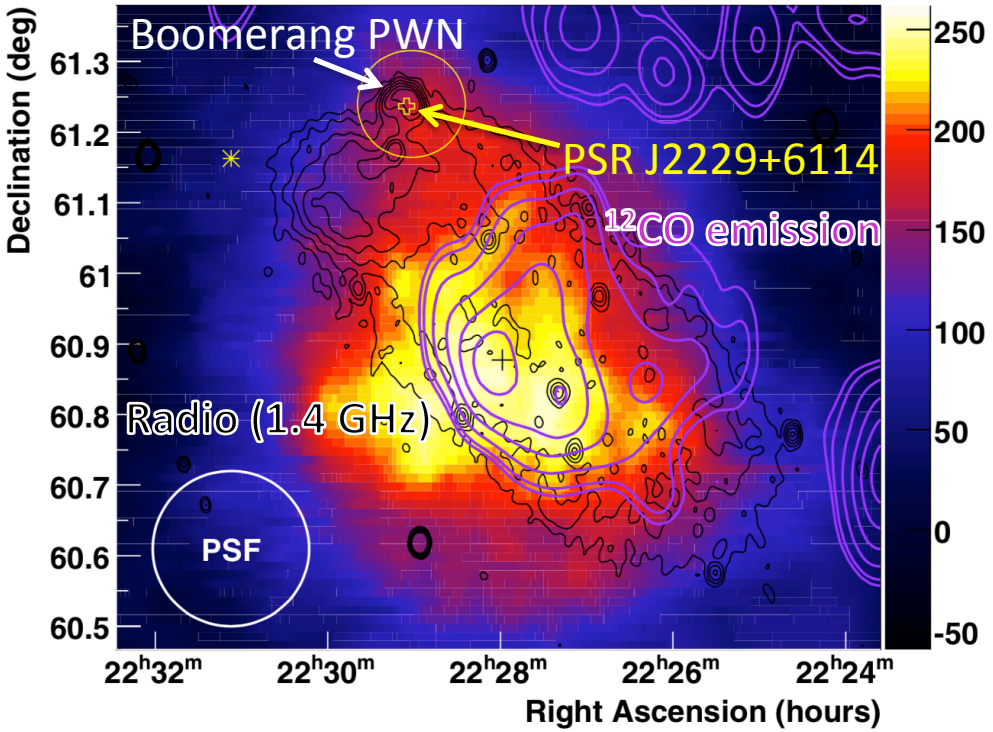

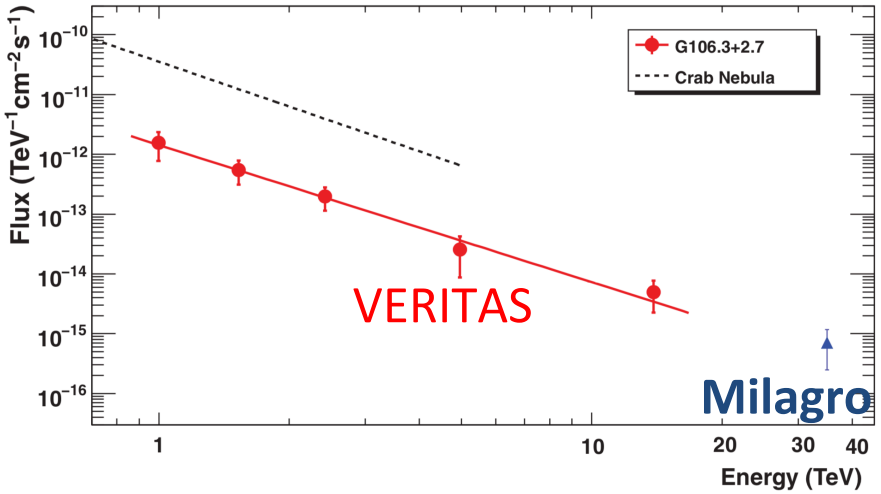

A. A. Abdo et al., ApJL, 700, L127 (2009)
V. A. Acciari et al., ApJL, 703, L6 (2009)

- age 10 kyr, distance 0.8 kpc, size 14 pc x 6 pc, if SNR is associated with Boomerang PWN *Kothes et al, ApJ, 560, 236 (2001)*
- At TeV energies, first observed by Milagro (MGRO J2228+61) and then by VERITAS (VER J2227+608)
- γ-ray emission centroid coincident with a molecular cloud
- spectrum seems to extend toward 35 TeV without cutoff

significance map by Tibet AS+MD

SNR G106.3+2.7

> 10 TeV

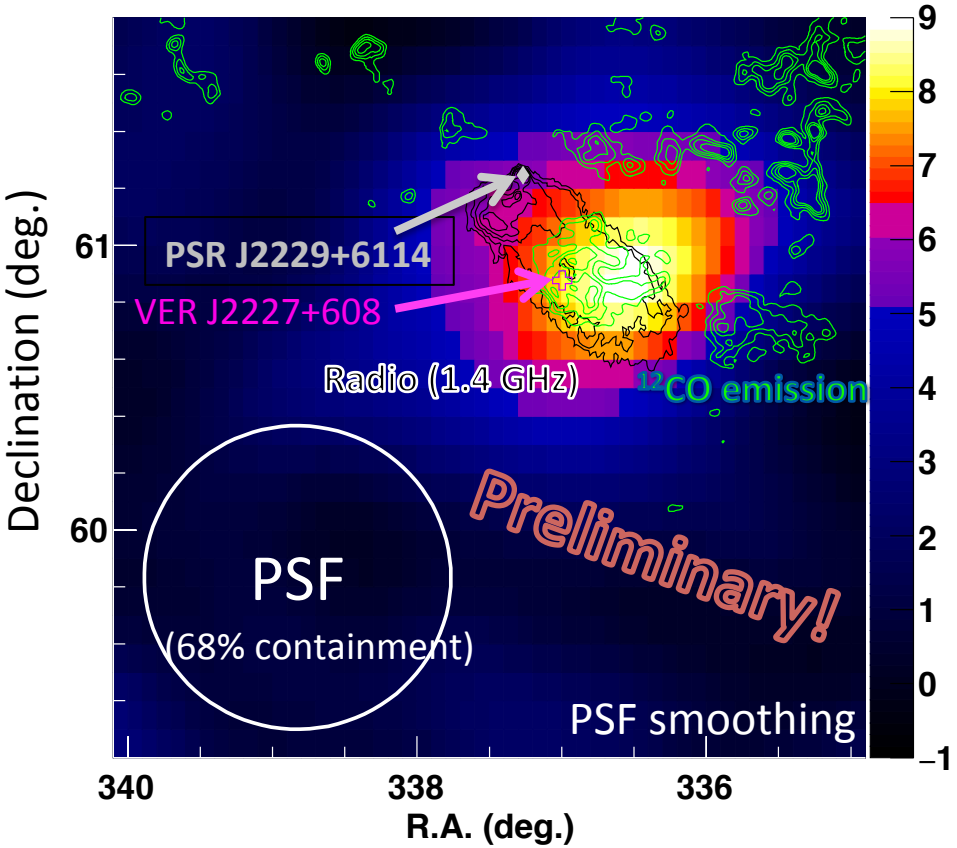

- Tibet emission centroid coincident with molecular cloud indicated by CO emission contours ※consistent with VERITAS
- spectrum under analysis

Summary

Crab Nebula & SNR G106.3+2.7 observed by Tibet AS+MD

- Muon cut by MD: ~99.9% CR rejection, ~90% γ efficiency @ 100 TeV

- Crab Nebula
  - **First Detection of Sub-PeV γ (5.6σ above 100 TeV)**
  - **Highest energy photon ~450 TeV *(See poster: PS1-75)***
  - spectrum consistent with IC model
  - spectrum consistent with HAWC results (3.3σ above 100 TeV)

- SNR G106.3+2.7
  - emission centroid > 10 TeV coincident with molecular cloud consistent with VERITAS
  - spectrum under analysis

Thank you for your attention!

Backup slides

Energy resolution

energy determined as a function of θ and $S50$ (particle density at 50m away from shower axis)

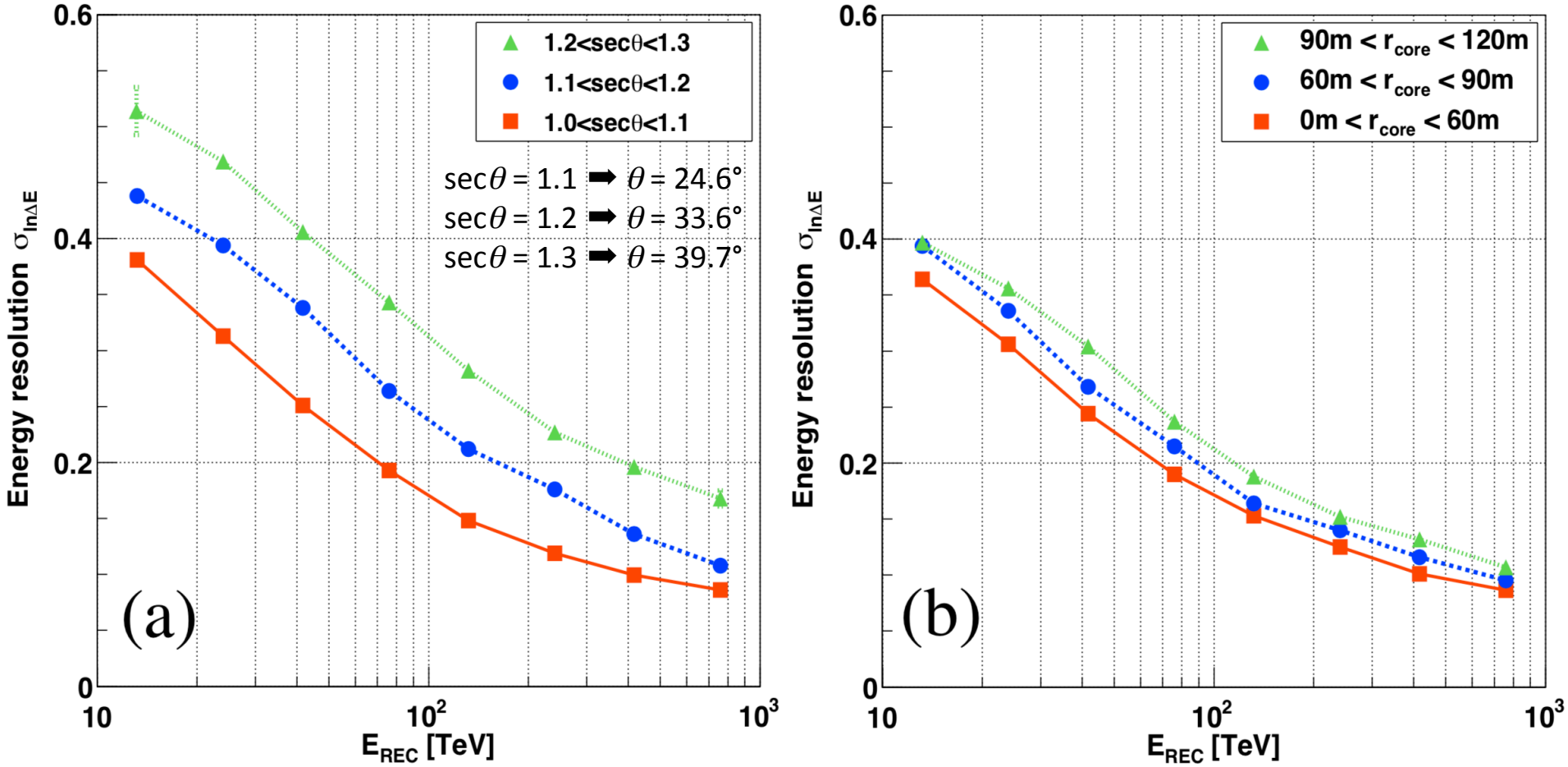

M. Amenomori et al., arXiv:1906.05521 (2019), Accepted by PRL

Crab: event list > 250 TeV

M. Amenomori et al., arXiv:1906.05521 (2019), Accepted by PRL

TABLE I. Probability of misidentifying cosmic-ray events from the Crab as a photon-like event ($P_{\rm CR}$) for each of four photon-like events above 250 TeV together with other reconstructed values. θ and $r_{\rm core}$ are the zenith angle and core distance from the AS array center, respectively.

E (TeV)	ΔE (TeV)	$\Sigma\rho$	ΣN_μ	θ (°)	$r_{\rm core}$ (m)	ϕ^2 (deg^2)	$P_{\rm CR}(>E)$
251	$^{+46}_{-43}$	3248	2.3	29.8	35.1	0.00	1.7×10^{-3}
313	$^{+58}_{-54}$	2440	5.5	27.5	94.6	0.03	2.2×10^{-2}
449	$^{+112}_{-97}$	2307	11.3	35.4	93.3	0.12	2.9×10^{-2}
458	$^{+83}_{-78}$	2211	21.5	27.5	111.6	0.18	0.23

If leptonic, where is the source of electrons?

Kothes et al., ApJ 560, 236 (2001)

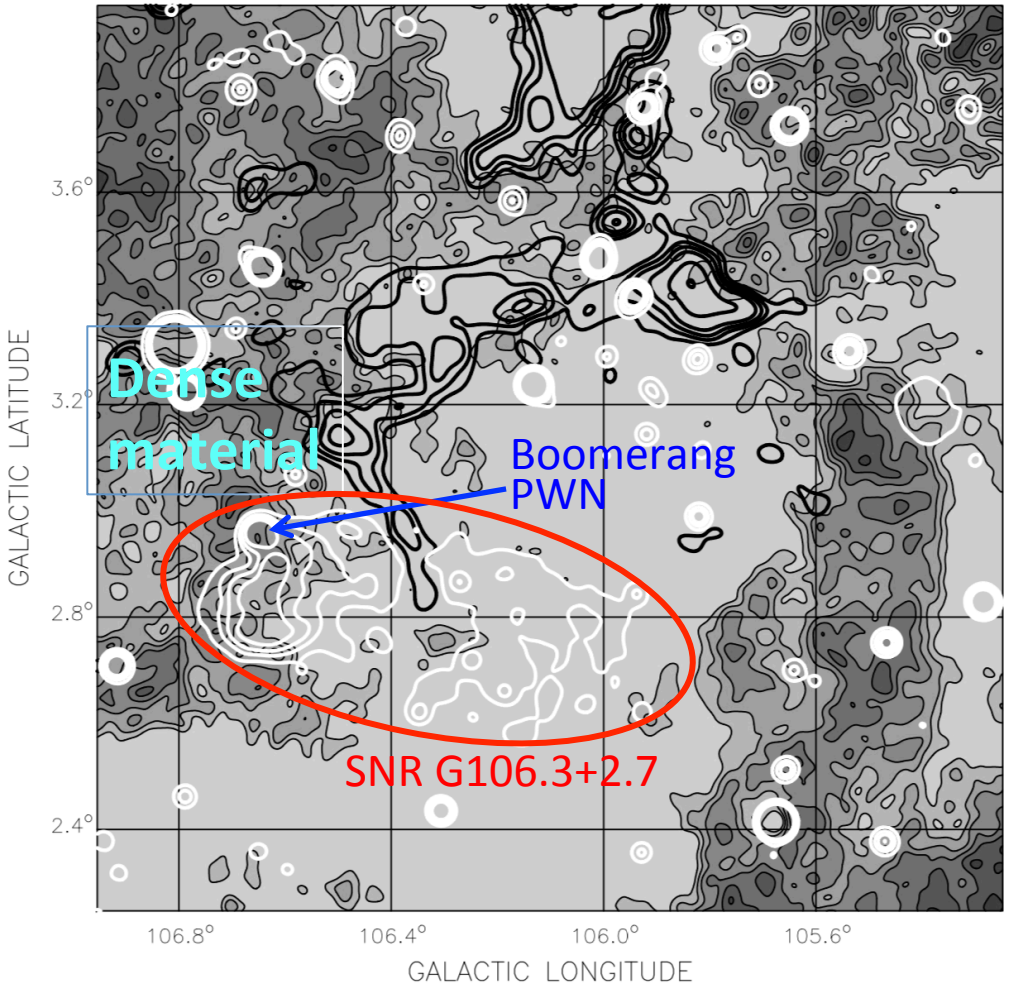

FIG. 5.—Gray-scale plot of neutral hydrogen associated with the SNR G106.3+2.7. Overlaid black contours represent molecular material and the white contours (at 200, 500, 800, and 1200 mK) show the radio continuum at 1420 MHz. All data have been convolved to a resolution of 2′ to improve the signal-to-noise ratio. For the neutral hydrogen and the CO, the three channels at −5.6, −6.4, and −7.2 km s^{-1} were averaged together.

Kothes et al, ApJ, 638, 225 (2006)

There is another plerion far below the Σ-$\dot{E}$-D relation as discussed by Kothes (1998). It is the youngest component of the PWN in G5.4−1.2. In this nebula the old electrons were displaced from the young electron population by the pulsar's high transverse velocity. This cannot be the case for the Boomerang, since Kothes et al. (2001) have shown that the pulsar's off center position was created not by a high transverse velocity but by the highly structured ambient medium. As shown by Blondin et al. (2001) for the Vela SNR, a density gradient can lead to an offset position of the pulsar from the center of the PWN, due to an asymmetric reverse shock. This should be observable in radio emission but not necessarily in X-rays, due to the short lifetime of the emitting electrons. In the case of the Boomerang, we are dealing with an extreme case of varying ambient density. The shock wave of the explosion, expanding to the north and east into the dense H I cloud discovered by Kothes et al. (2001), was decelerated very quickly, and a strong reverse shock moved toward the interior. The reverse shock blew the PWN into the opposite direction, where the shock wave was expanding into moderately dense material. After passage of the reverse shock, the pulsar created another wind nebula, although with much less energy input than before. To the north and east this nebula is confined by the wall that also stopped the supernova shock wave in that direction. To the south and west the area is almost empty; there the wind nebula is dispersing smoothly into this low-density cavity. From the relation between the age of the nebula and the magnetic field inside the nebula (see § 4.1), we know that this phase started about 3900 yr ago. At that time, the characteristic age of the pulsar would have been 6560 yr, which would also have been the lifetime of the Boomerang.

$[P/(2\dot{P})] = 10,460$ yr. Kothes et al. (2001) associated this pulsar and its synchrotron nebula with the SNR G106.3+2.7 and derived a distance of 800 pc for both objects on the basis of linear polarization measurements, foreground H I column density, and associated H I and CO. The exceptionally low radio luminos-

G106.3+2.7: observation by Milagro

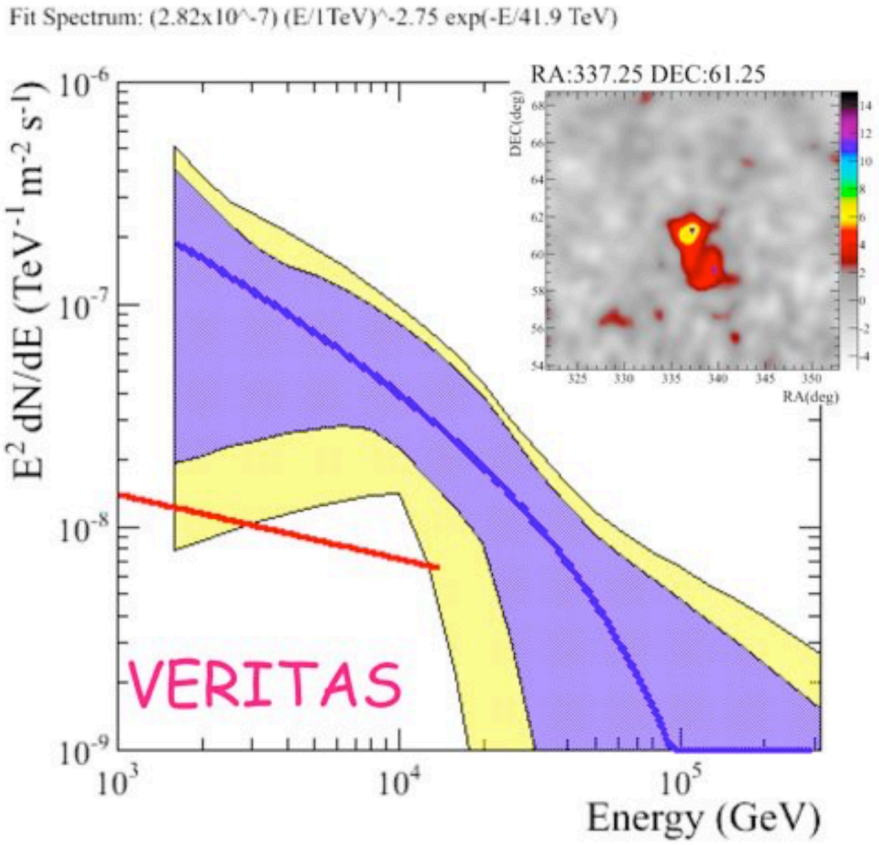

Figure 5 Spectrum of PSR 2229+6114. The Spectrum measured by VERITAS has been overlaid (red line).

Figure 5 shows the spectrum for PSR J2229+6114. Milagro detects this source at 6.6σ. This source, as the others can be adequately fit to either a soft spectrum with no cutoff or a hard spectrum with a cutoff at or above 10 TeV. This source was also reported by VERITAS [30]. The spectrum reported by VERITAS is shown on the figure and is consistent with the Milagro measured spectrum with errors. The spectral index reported by VERITAS has a sufficiently large error that, unlike the case of PSR J1908+06, we cannot use the IACT spectral index measurement to constrain the Milagro fit and definitively rule in or out the presence of a high energy cutoff.

emission centroid
(R.A., Dec) = (337.18°, 61.17°)
error 0.165°

※consistent with VERITAS

A. J. Smith et al., arXiv:1001.3695 (2010)